J Mater Sci: Mater Electron (2014) 25:2053–2059
DOI 10.1007/s10854-014-1839-9

Enhanced photocatalytic activity of $Mg_{0.05}Zn_{0.95}O$ thin films prepared by sol–gel method through a cycle

Zhitao Zhou · Fengjiao Shang · Guangcai Pan · Feng Wang · Changlong Liu · Wanbing Gong · Zhenfa Zi · Yiyong Wei · Jianguo Lv · Xiaoshuang Chen · Gang He · Miao Zhang · Xueping Song · Zhaoqi Sun

Received: 18 January 2014 / Accepted: 25 February 2014 / Published online: 5 March 2014

Abstract $Mg_{0.05}Zn_{0.95}O$ thin films were prepared on silicon substrates by a sol–gel dip-coating technique. Microstructure, surface topography and optical properties of the thin films were characterized by X-ray diffraction, atom force microscopy, Fourier transform infrared spectrophotometer and fluorescence spectrometer. The results show that the thin film annealed at 700 °C has the largest average grain size and exhibits the best *c*-axis preferred orientation. As annealing temperature increases to 800 °C, the grain along *c*-axis has been suppressed. Roughness factor and average particle size increase with the increase of annealing temperature. The IR absorption peak appearing at about 416 cm^{-1} is assigned to hexagonal wurtzite ZnO. The thin film annealed at 700 °C has the maximum oxygen vacancy, which can be inferred from the green emission intensity. Photocatalytic results show that the thin film annealed at 700 °C exhibits remarkable photocatalytic activity, which may be attributed to the larger grain size, roughness factor and concentration of oxygen vacancy. Enhanced photocatalytic activity of $Mg_{0.05}Zn_{0.95}O$ thin films after a cycle may be attributed to the increase of surface oxygen vacancy and photocorrosion of amorphous MgO on the surface of thin film under UV irradiation.

Z. Zhou · F. Shang · G. Pan · F. Wang · C. Liu · W. Gong · Z. Zi · Y. Wei · J. Lv (✉)
School of Electronic and Information Engineering, Hefei Normal University, Hefei 230061, China
e-mail: lvjg1@163.com

C. Liu · J. Lv · X. Chen (✉)
National Laboratory for Infrared Physics, Shanghai Institute of Technical Physics, Chinese Academy of Sciences, Shanghai 200083, China
e-mail: xschen@mail.sitp.ac.cn

J. Lv · G. He · M. Zhang · X. Song · Z. Sun (✉)
School of Physics and Material Science, Anhui University, Hefei 230039, China
e-mail: szq@ahu.edu.cn

1 Introduction

The hazardous wastes related to industrial activities, including toxic contaminated air and organic wastewater have resulted in serious worldwide environmental problems [1–5]. Photocatalysis is widely used for the removal of harmful organic contaminants from water and air under UV or solar light irradiation. Various metal oxide semiconductors such as TiO_2, ZnO, WO_3 and SnO_2 have been studied as photocatalyst. Among of them, ZnO is one of the potential candidates due to its high photocatalytic efficiency, inexpensive material and environmentally friendly. The photocatalytic activity of ZnO, which were prepared by a variety of methods such as sonochemical method [6], sputtering [7], sol–gel method [8], hydrothermal method [9], spray pyrolysis [10], solvothermal method [11], has been studied. So far, there are many reports on the investigations of the photocatalytic activity of ZnO powders. The photocatalytic activity of ZnO thin films have been reported seldom. However, in a continuous flow system such as in wastewater treatment, these photocatalysts in form of powder are not easy to separate and recycle. In order to overcome these problems, more attentions have been focused on ZnO thin films so as to reduce the difficult and expensive process for the separation and recycling of the ZnO powders.

Unfortunately, a drawback for the ZnO photocatalyst is its photoinstability in aqueous solution due to its photocorrosion effect, which significantly decreases its photocatalytic activity and limits its practical applications.

Recently, several methods have been developed to improve its photostability, including surface coating and surface hybridization [12, 13]. Wang et al. [12] reported that the Ag modified ZnO/SiO_2 hierarchical structures shows enhanced photocatalytic efficiency and satisfactory recycling ability. Zhang et al. [13] thought that the photocatalytic activity of ZnO can be been enhanced by hybridization with carbon layers, which can improve the adsorption ability and suppress the coalescence and crystal growth of ZnO nanoparticles after thermal treatment. However, different methods and attempts to increase the photocatalytic activity and photostability of ZnO will still need more detailed studies.

In this letter, $Mg_{0.05}Zn_{0.95}O$ thin films were prepared by sol–gel method. Effects of annealing temperature on the microstructure, surface topography, optical properties and photocatalytic activity of the thin films were investigated. Enhanced photocatalytic activity of the thin films through a cycle has been studied in detail.

2 Experiments

2.1 Preparation and characterization

2-Methoxyethanol [$CH_3OCH_2CH_2OH$] and mono-ethanolamine (MEA) were used as the solvent and stabilizing agent, respectively. 8.32 g zinc acetate dehydrate [$Zn(CH_3COO)_2{\cdot}2H_2O$] and 0.43 g magnesium acetate tetrahydrate [$Mg(CH_3COO)_2{\cdot}\ 4H_2O$] were dissolved in 2-methoxyethanol, and then MEA was added to the solution. The molar ratio of Mg/Zn was 0.05/0.95. The concentration of metal ions in $Mg_{0.05}Zn_{0.95}O$ sols was 0.5 M and the molar ratio of MEA to metal ions was kept at 1:1. The solution was stirred at 60 °C for 2 h using a magnetic stirrer to get a clear, homogeneous and transparent sol, which served as the coating sol after being kept for 24 h. The double polished silicon substrates (15 × 15 mm) were cleaned ultrasonically in acetone and distilled water for 10 min, respectively. The $Mg_{0.05}Zn_{0.95}O$ thin film was deposited on silicon substrates using a spin coating method. The spinning speed and time were 3,000 rpm and 30 s, respectively. After each spin coating, the substrates were kept at 150 °C for 10 min to evaporate the solvent and remove organic residuals in the thin film. The procedure was repeated 10 times. The films were annealed in air at 500, 700 and 800 °C for 60 min, respectively.

Crystallinity was analyzed by X-ray diffraction (XRD, MACM18XHF) with Cu Kα radiation (λ = 0.15405 nm). The accelerated voltage and applied current were 100 kV and 40 mA, respectively. Surface topography was characterized by atom force microscopy (AFM, CSPM4000) operating in contact mode with a scanning area of 3,000 × 3,000 nm. IR transmission spectrum was measured by Fourier transform infrared (FTIR, BRUKER VERTEX 80) spectrophotometer over the range 4,000–400 cm^{-1}. The photoluminescence spectrum was examined at room temperature by fluorescence spectrometer (FL, HITACHI F-4500) with a xenon lamp as light source operating at 325 nm.

2.2 Photocatalytic activity

The photocatalytic activity of the $Mg_{0.05}Zn_{0.95}O$ thin films was estimated by the photodegradation of methyl orange (MO) aqueous solution with an initial concentration of 5 ppm (mg/L). A 36 W low mercury lamp (λ = 254 nm) was used as light source. $Mg_{0.05}Zn_{0.95}O$ thin films with a dimension of 15 × 15 mm were immersed into 5 mL of the above MO solution in a beaker. The distance between UV lamp and the film surface was 10 cm. At given time intervals, UV–Vis absorption spectrum of MO was recorded by UV–Vis spectrophotometer (UV–Vis, TU1900). The degradation efficiency of different thin film was determined by UV–Vis spectrum at its maximum absorption wavelength of 464 nm. The absorbance of methyl orange at 464 nm is proportional to concentration. According to the standard curve between concentration and absorbance, the value of $(1-C_t/C_0) \times 100$ % was calculated, denoted as the degradation efficiency. C_o and C_t are the initial and residual MO concentration after t min reaction. Similar procedures were conducted three times to evaluate the enhanced recycling photocatalytic ability.

3 Results and discussion

Figure 1 shows the XRD patterns of $Mg_{0.05}Zn_{0.95}O$ thin films annealed at 500, 700, and 800 °C. It is seen that the nine diffraction peaks at $2\theta = 31.77°$, 34.42°, 36.25°, 47.54°, 56.60°, 62.86°, 66.37, 67.96°, and 69.09° in this XRD patterns match well with (100), (002), (101), (102), (110), (103), (200), (112)and (201) directions of hexagonal wurtzite ZnO (JCPDS 36-1451), respectively. Even if the temperature is as high as 800°, no peaks corresponding to either Mg metal or any of its oxides have been observed in the patterns, which indicate that Mg ions have incorporated into the ZnO host lattice. Average grain size D of the thin films were calculated by means of Scherrer's formula [14]

$$D = 0.9\lambda/\beta\cos\theta \quad (1)$$

where λ is the X-ray wavelength, β is the peak width at half height of the diffraction peaks, and θ is the diffraction angle. The average grain size of the thin films are listed in Table 1. It can be seen that the thin film annealed at 700 °C

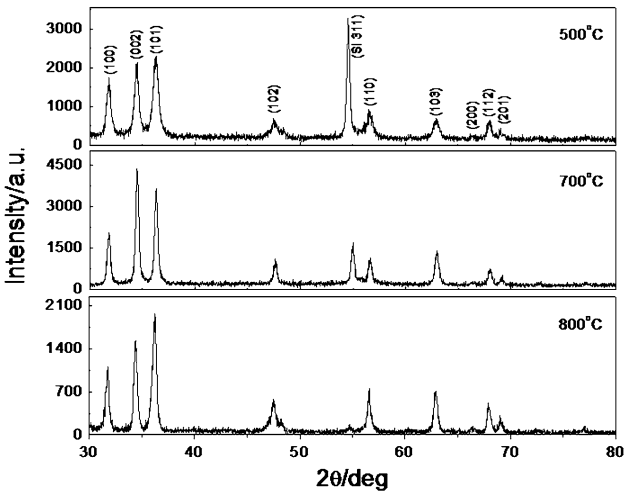

Fig. 1 XRD patterns of $Mg_{0.05}Zn_{0.95}O$ thin films annealed at different temperature

has the largest average grain size and exhibits the best *c*-axis preferred orientation. The results indicate that 700 °C is the optimal annealing temperature. As annealing temperature increases to 800 °C, the grains along *c*-axis have been suppressed.

Figure 2 shows AFM images of $Mg_{0.05}Zn_{0.95}O$ thin films with different annealing temperature. It can be seen that the $Mg_{0.05}Zn_{0.95}O$ thin film annealed at 500 °C consists of a large number of uniform small particles. Surface RMS roughness and roughness factor *r* [15], which is defined as the ratio of the actual area of a rough surface to the geometric projected area, were calculated by means of Imager software. The results are listed in Table 1. It can be seen that as annealing temperature increases, surface RMS roughness increases from 2.1 nm to 14.0 nm, *r* value increases from 1.005 to 1.035, and average particle size increases from 71 to 264 nm. The results indicate that the RMS roughness of the thin films are related to roughness factor and average particle size.

Figure 3 shows the IR transmission spectra of $Mg_{0.05}Zn_{0.95}O$ thin films with different annealing temperature. The absorption peak appears at about 416 cm^{-1}, which comes from Zn–O stretching vibration, is assigned to hexagonal wurtzite ZnO [16]. The absorption peak around 1,072 cm^{-1} is attributed to Si–O–Si asymmetric stretching vibration [17]. The increase of the absorbance peak may be attributed to the increase of SiO_2 on the interface of silicon and sample with the increase of annealing temperature. The peak at about 1,600 cm^{-1} is assigned to bending vibrations of H–O–H bonds. The decrease of this peak indicates that moisture on the thin films decrease with the increase of annealing temperature. The peak at near 2,348 cm^{-1} is attributed to asymmetrical stretch of C–O which comes from CO_2 on the thin film surface or in the air during the testing process. The peak at about 2,923 cm^{-1} is assigned to low frequency absorption peak of C–H stretching vibration.

Figure 4 shows the PL spectra of $Mg_{0.05}Zn_{0.95}O$ thin films with different annealing temperature. A near band edge (NBE) emission band and a green emission band have been observed in all thin films, but the intensity ratio of green emission to NBE emission is different. Wang et al. [18] reported that the UV emission with a peak at 380 nm may be attributed to the free exciton emission. Gao et al. [19] believed that the UV emission located at 391 nm originated from the electron transition from the localized levels below the conduction band to the valance band. The formation of the localized levels was related to the free impurity atoms, various defects, surface and interface. Wang et al. [20] thought that the violet emission (402 nm) was ascribed to the electron transition from the conduction band tail states to the valence band tail states. Therefore, the origins of NBE emission of the thin films may be attributed to the exciton recombination between the electrons in the conduction band and the holes in the valence band. The red shift of the NBE emission peak with increasing annealing temperature may be attributed to appearance of the localized levels below the conduction band. It can be seen that the intensity of green emission increases first and then decreases with the increase of annealing temperature. Generally, the green emission band is attributed to oxygen vacancy [18]. The change of green emission intensity indicated a change of the number of oxygen vacancy. It can be concluded that the $Mg_{0.05}Zn_{0.95}O$ thin film annealed at 700 °C has the maximum oxygen vacancy.

The photocatalytic activity in this work is evaluated from two aspects: the photocatalytic degradation efficiency and the recycling ability. Figure 5 shows time dependent

Table 1 Average grain size, RMS, *r*, degradation efficiency of $Mg_{0.05}Zn_{0.95}O$ thin films annealed at different temperature

Annealing temperature (°C)	Average grain size (nm)	RMS (nm)	*r*	Degradation efficiency		
				First recycle	Second recycle	Third recycle
500	17.2	2.1	1.005	63.9	76.1	76.4
700	26.8	12.1	1.022	78.1	80.6	82.2
800	25.1	14.0	1.035	20.8	42.2	45.0

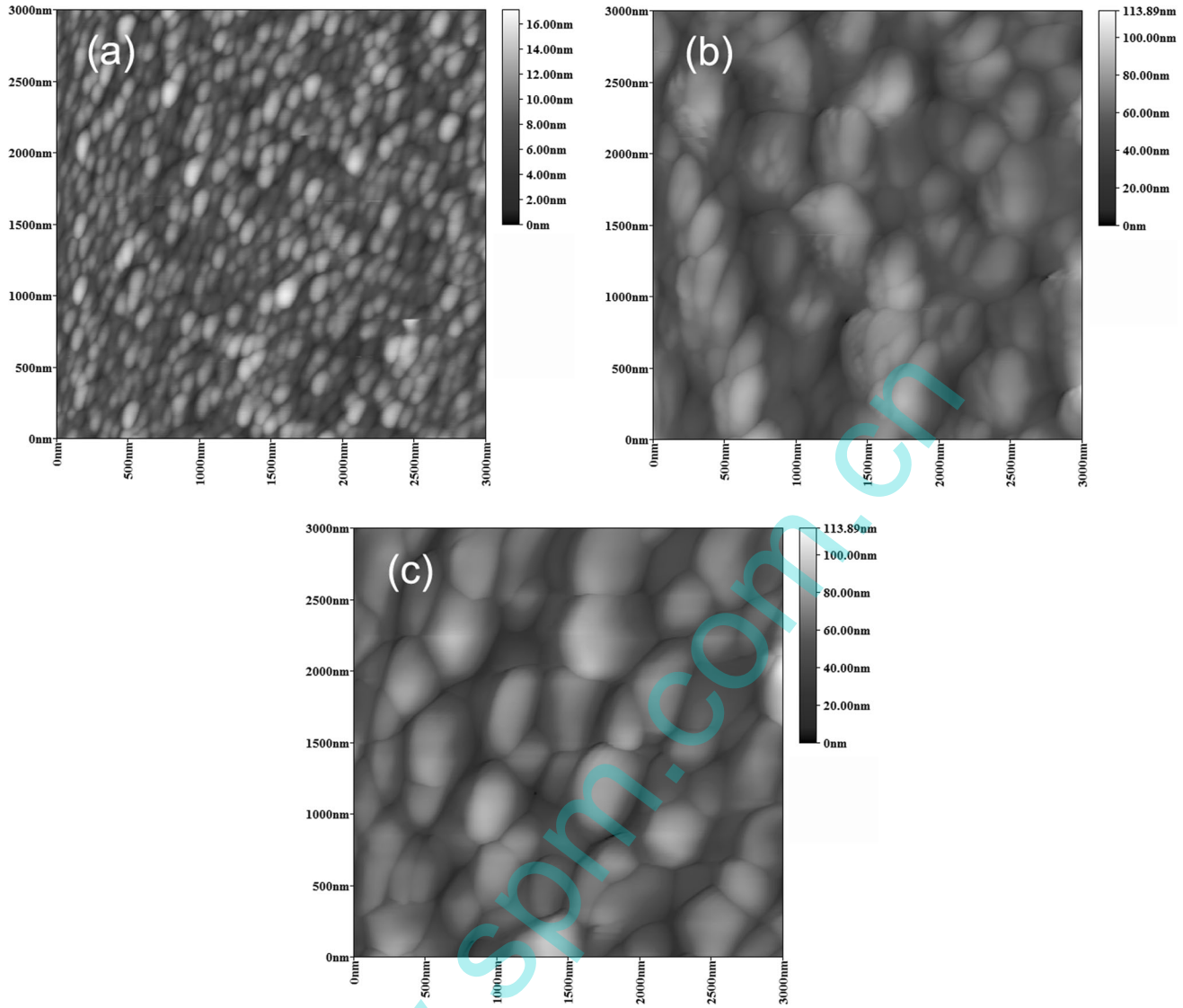

Fig. 2 AFM images of $Mg_{0.05}Zn_{0.95}O$ thin films annealed at **a** 500 °C, **b** 700 °C, **c** 800 °C

UV absorption spectra of MO in the presence of $Mg_{0.05}Zn_{0.95}O$ thin film annealed at 700 °C. Figure 6 shows the curves of C_t/C_0 versus irradiation time using $Mg_{0.05}Zn_{0.95}O$ thin film annealed at different temperature and without thin film. The photocatalytic degradation efficiency of MO using the thin films after 180 min UV irradiation is listed in Table 1. It can be seen that the direct photolysis of MO is ineffective ($\sim$10 %) after a reaction time of 180 min. The thin films annealed at 700 and 800 °C exhibit remarkable and poor photocatalytic activity, respectively. The thin film annealed at 700 °C shows the better photocatalytic activity than that of other thin films. The remarkable photocatalytic activity of the thin film can be explained as follows. The photocatalytic efficiency of ZnO thin films could be enhanced by improving the grain size [21]. The surface area is another important parameter that can improve the photocatalytic activity of the ZnO. The better photocatalytic activity may be due to the enhancement in surface area might increase the reactant adsorption [22]. The larger surface defects such as oxygen vacancies, which benefit the efficient separation of electron–hole pairs and minimize the radiative recombination of electron and hole after UV irradiation [23]. Therefore, the thin film annealed at 700 °C exhibits remarkable photocatalytic activity may be attributed to the larger grain size, roughness factor and concentration of oxygen vacancy. The thin film annealed at 800 °C shows the poor photocatalytic activity is due to the increase of amorphous MgO on the surface of thin film as annealing temperature increase [24].

It was reported that ZnO suffers from a considerable decrease of its photocatalytic activity due to the photocorrosion when it was recycled for the photodegradation of

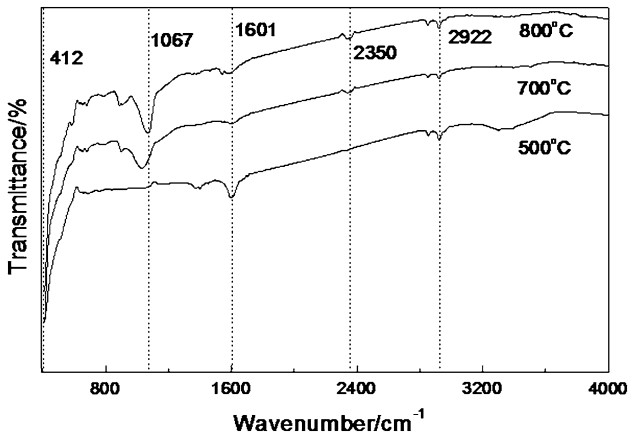

Fig. 3 FTIR spectra of $Mg_{0.05}Zn_{0.95}O$ thin films annealed at different temperature

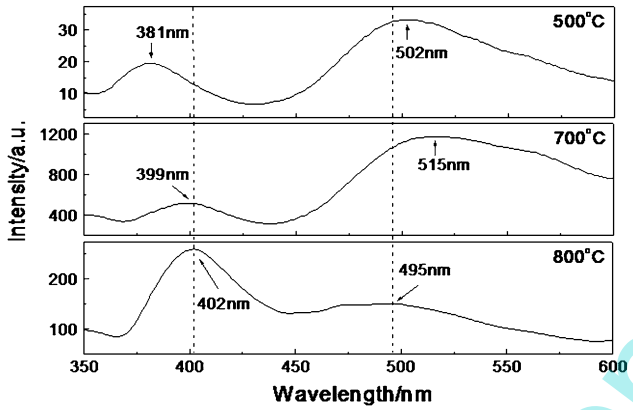

Fig. 4 PL spectra of $Mg_{0.05}Zn_{0.95}O$ thin films annealed at different temperatures

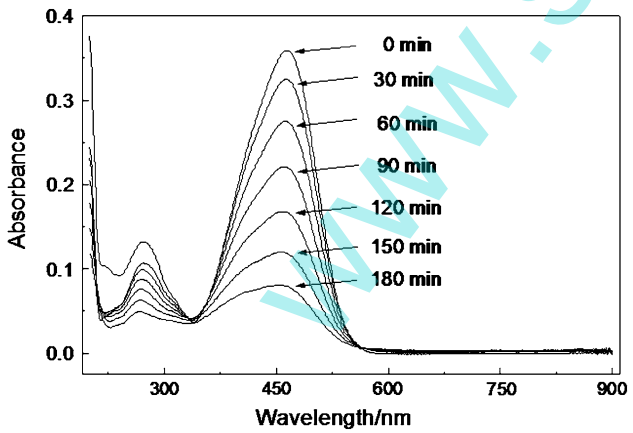

Fig. 5 Time dependent UV absorption spectra of MO in the presence of $Mg_{0.05}Zn_{0.95}O$ thin film annealed at 700 °C

various dyes [12, 25]. Therefore, the recycling ability is one of important properties to estimate the photocatalytic performance of ZnO. Figure 7a, b and c show the recycling

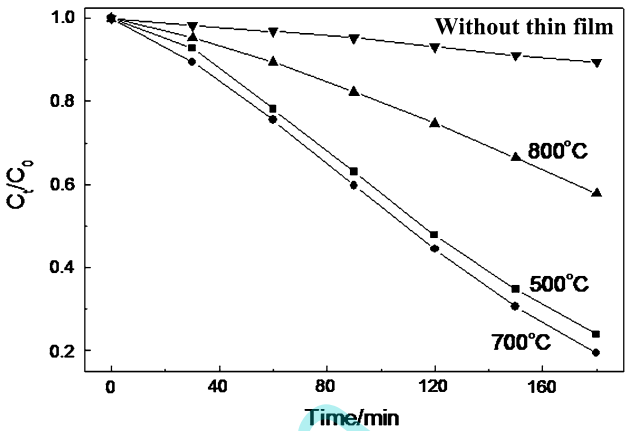

Fig. 6 Curves of C_t/C_0 versus irradiation time with and without $Mg_{0.05}Zn_{0.95}O$ thin films

test results for the $Mg_{0.05}Zn_{0.95}O$ thin films annealed at 500, 700 and 800 °C, respectively. The photocatalytic degradation efficiency for the second and third recycles are listed in Table 1. It can be seen that the photocatalytic degradation efficiency of the $Mg_{0.05}Zn_{0.95}O$ thin films increases gradually after three successive recycles. The enhanced recycling ability of $Mg_{0.05}Zn_{0.95}O$ thin films is in striking contrast to the photoinstability of ZnO.

The photocorrosion of ZnO is due to the ZnO is photooxidized to Zn^{2+} and O_2 by photogenerated holes under light irradiation. When ZnO is subjected to intrinsic excitation, electrons are promoted from the valence band to the conduction band and generating electron–hole pairs. The holes are transported to the ZnO surface and inclined to undergo a reaction with the surface oxygen atom, resulting in the escape of oxygen from the surface. The process of photocorrosion consumes some photoinduced holes, which damage the photocatalytic activity of ZnO. Furthermore, the crystal structure of ZnO collapses, and loses the activity for the degradation ultimately [26]. In order to enhance the photostability, many efforts have been employed to suppress the photocorrosion of ZnO. Fu et al. [25] acquired photostable hybrid photocatalyst of C60/ZnO by anchoring fullerenes C60 molecule on the surface defect sites of ZnO, which substantially reduced the activation of the surface oxygen atom, and effectively inhibited the photocorrosion of ZnO. Li et al. [27] though that the phenolic compounds can form a surface complex with ZnO. The photogenerated holes trapped on the surface of ZnO probably prefer reacting with the surface complex to reacting with the surface oxygen atom. Consequently, the formation of the surface complex results in an improvement of the photostability of ZnO. In this letter, UV irradiation results in a considerable increase of surface oxygen vacancy after a cycle, which increases the photocatalytic

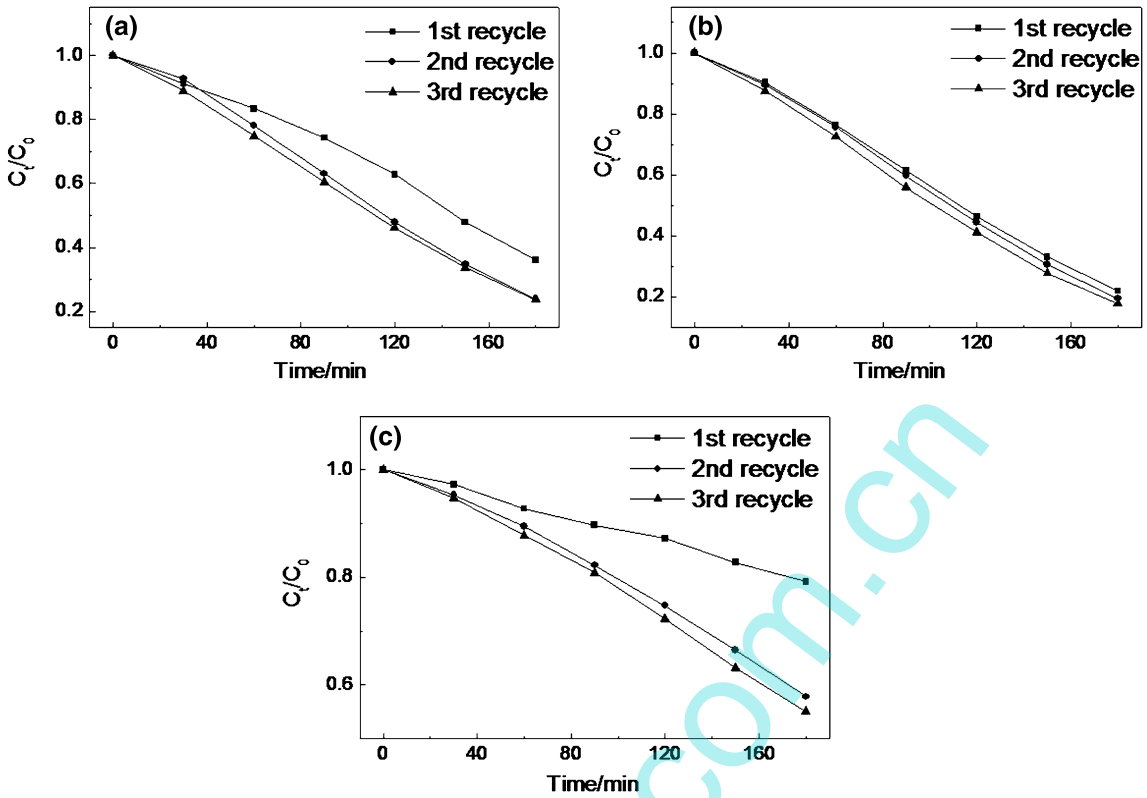

Fig. 7 Recycling test results for the $Mg_{0.05}Zn_{0.95}O$ thin films annealed at **a** 500 °C, **b** 700 °C and **c** 800 °C, respectively

activity of the thin films and enhances its recycling ability. On the other hand, UV irradiation results in photocorrosion of amorphous MgO on the surface of thin films, which increase the interface of ZnO and MO aqueous solution and enhance the photocatalytic activity after a cycle.

4 Conclusions

Microstructure, surface topography, optical and photocatalytic properties of $Mg_{0.05}Zn_{0.95}O$ thin films deposited on silicon substrates via sol–gel method were investigated. The thin film annealed at 700 °C exhibits the best *c*-axis preferred orientation. As annealing temperature increases from 500 to 800 °C, surface RMS roughness increases from 2.1 to 14.0 nm and roughness factor increases from 1.005 to 1.035. The absorption peak appears at about 416 cm^{-1} is assigned to Zn–O stretching vibration. The increase of the absorbance peak around 1,072 cm^{-1} can be attributed to the increase of SiO_2 on the interface of silicon and sample with the increase of annealing temperature. It can be concluded from PL spectra that the thin film annealed at 700 °C has the maximum oxygen vacancy. Photocatalytic activity the $Mg_{0.05}Zn_{0.95}O$ thin film is related to grain size, roughness factor and concentration of oxygen vacancy. The improvement of photocatalytic activity through a cycle may be related to the increase of surface oxygen vacancy and photocorrosion of amorphous MgO under UV irradiation.

Acknowledgments This work was supported by State Key Program for Basic Research of China (2013CB632705), National Natural Science Foundation of China (Nos. 11334008, 61290301, 51072001, 51272001, 51002156, 51102072), China Postdoctoral Science Foundation (No. 2012M520944), Anhui Provincial Natural Science Foundation (Nos. 1208085MF99, 1208085QA16), Natural Science Foundation of Anhui Higher Education Institution of China (No. KJ2012Z336), Shanghai Postdoctoral Science Foundation (No. 12R21416800), Funds for Distinguished Young Scholar of Anhui University (No. KJJQ1103).

References

1. X. Fang, T. Zhai, U.K. Gautam, L. Li, L. Wu, Y. Bando, D. Golberg, Prog. Mater. Sci. **56**, 175–287 (2011)
2. D. Hao, Z. Yang, C. Jiang, J. Zhang, J. Mater. Sci. Technol. **29**, 1074–1078 (2013)
3. X. Fang, L. Wu, L. Hu, Adv. Mater. **23**, 585–598 (2011)
4. L. Peng, L. Hu, X. Fang, Adv. Funct. Mater. (2014). doi:10.1002/adfm.201303367
5. S. Chakrabarti, S. Kar, A. Dev, S. Chaudhuri, Phys. Status Solidi A **202**, 441–448 (2005)
6. O. Yayapao, T. Thongtem, A. Phuruangrat, S. Thongtem, J. Alloys Compd. **576**, 72–79 (2013)
7. Y. Liu, N. Zhao, W. Gao, RSC Adv. **3**, 21666–21674 (2013)

8. J.B. Zhong, J.Z. Li, Z.H. Xiao, W. Hu, X.B. Zhou, X.W. Zheng, Mater. Lett. **91**, 301–303 (2013)
9. Y. Fang, Z. Li, S. Xu, D. Han, D. Lu, J. Alloys Compd. **575**, 359–363 (2013)
10. M. Bizarro, A. Sanchez-Arzate, I. Garduno-Wilches, J.C. Alonso, A. Ortiz, Catal. Today **166**, 129–134 (2011)
11. P. Gu, X. Wang, T. Li, H. Meng, Mater. Res. Bull. **48**, 4699–4703 (2013)
12. R. Wang, J. Guo, D. Chen, Y.-E. Miao, J. Pan, W.W. Tjiu, T. Liu, J. Mater. Chem. **21**, 19375–19380 (2011)
13. L. Zhang, H. Cheng, R. Zong, Y. Zhu, J. Phys. Chem. C **113**, 2368–2374 (2009)
14. H. Chen, J. Ding, S. Ma, Phys. E **42**, 1487–1491 (2010)
15. C. Sun, L.-Q. Ge, Z-.Z. Gu, Thin Solid Films **515**, 4686–4690 (2007)
16. T. Ivanova, A. Harizanova, T. Koutzarova, B. Vertruyen, J. Non-Cryst. Solids **357**, 2840–2845 (2011)
17. J. Hnilica, J. Schäfer, R. Foest, L. Zajíčková, V. Kudrle, J. Phys. D Appl. Phys. **46**, 335202–335208 (2013)
18. M. Wang, K.E. Lee, S.H. Hahn, E.J. Kim, S. Kim, J.S. Chung, E.W. Shin, C. Park, Mater. Lett. **61**, 1118–1121 (2007)
19. X.D. Gao, X.M. Li, W.D. Yu, J. Solid State Chem. **177**, 3830–3834 (2004)
20. Q.P. Wang, D.H. Zhang, Z.Y. Xue, X.T. Hao, Appl. Surf. Sci. **201**, 123–128 (2002)
21. P. Jongnavakit, P. Amornpitoksuk, S. Suwanboon, T. Ratana, Thin Solid Films **520**, 5561–5567 (2012)
22. L. Zhang, L. Yin, C. Wang, N. Lun, Y. Qi, ACS Appl. Mater. Interfaces **2**, 1769–1773 (2010)
23. J. Wang, P. Liu, X. Fu, Z. Li, W. Han, X. Wang, Langmuir **25**, 1218–1223 (2009)
24. S. Suwanboon, P. Amornpitoksuk, P. Bangrak, N. Muensit, Ceram. Int. **39**, 5597–5608 (2013)
25. H. Fu, T. Xu, S. Zhu, Y. Zhu, Environ. Sci. Technol. **42**, 8064–8069 (2008)
26. S. Meng, D. Li, X. Zheng, J. Wang, J. Chen, J. Fang, Y. Shao, X. Fu, J. Mater. Chem. A **1**, 2744–2747 (2013)
27. Y. Li, X. Zhou, X. Hu, X. Zhao, P. Fang, J. Phys. Chem. C **113**, 16188–16192 (2009)